

SHORTER COMMUNICATIONS

THE EFFECT OF PORE-SHAPE, -CONFIGURATION AND -ORIENTATION ON THE THERMAL CONDUCTIVITY OF POROUS MATERIALS

I. I. SHERIF, A. S. A. AMMAR and S. A. EL-MESSIH

Physics Department, Faculty of Engineering, Alexandria University, Egypt

(Received 19 August 1974 and in revised form 28 February 1975)

NOMENCLATURE

A ,	sample cross-section ($= 4.372 \times 10^{-4} \text{ m}^2$);
d ,	sample thickness;
K ,	apparent thermal conductivity;
P ,	porosity (volume fraction of the gas phase);
P_s ,	volume fraction of the solid phase;
S ,	surface area of the heat sink ($= 0.303 \times 10^{-2} \text{ m}^2$);
T_0 ,	wall temperature of the surrounding evacuated chamber;
T_1 ,	temperature of the heat source;
T_x ,	temperature of the heat sink;
V ,	volume of the disk;
V_g ,	volume of the gas phase;
V_s ,	volume of the solid phase;
W ,	weight of the disk;
W_g ,	weight of the gas phase;
W_s ,	weight of the solid phase.

Greek symbols

ρ_a ,	apparent density of the sample;
ρ_s ,	true density of the solid material ($= 4.488 \times 10^3 \text{ kg} \cdot \text{m}^{-3}$);
σ ,	Stefan's constant ($= 5.67 \times 10^{-8} \text{ W} \cdot \text{m}^{-2} \cdot \text{deg}^{-4}$);
ϵ ,	emissivity of the heat sink ($= 0.95 \pm 0.01$).

INTRODUCTION

THE IMPORTANCE of the study of thermophysical properties of porous materials comes from the fact that industrial materials are mostly of porous nature. Such bodies are composed of pure materials with different proportions. Most of porous materials used in industry could be considered as two phase systems. One of these is the solid material while the other is a gas phase (mostly air). Any thermophysical property, for such system, beside depending on the properties of each phase must also depend on: the volumetric proportions of the phases with respect to each other, the grain size of the different phases, and on the distribution of such grain sizes in the body. One of the most important properties, especially in the case of refractory materials, is the thermal conductivity. Practically speaking, since each phase within the body contributes to the thermal conductivity, then any measured conductivity is an apparent one. The problem of the prediction of the apparent thermal conductivity is of great importance in practical applications. Various correlations have been reported in the literature for this purpose. One of these correlations is that derived by Eucken [1], who showed the influence of the pores for a volume of two phase system. Sherif [2], rearranging Eucken's equation represented the relation between the apparent conductivity and the bulk density as a vertical parabola.

Deissler and Boegil [3], suggested that, by using heat conduction together with statistical method, one might obtain an expression for K which accounts for irregular arrangement and shape of the particles. The most recent work for prediction of the effective thermal conductivity of porous materials for two phase systems for randomly

sized and distributed particles based on a statistical approach is the work of Cheng and Vachon [4].

The present work is concerned with experimental measurements of the apparent thermal conductivity of titanium oxide powder manufactured in the form of small disks having different porosities covering the porosity range from about 50 to about 70 per cent. Measurements showed that the correlations for the prediction of the thermal conductivity, reported in the literature, would depart from the experimental values and the degree of such departure depends on the range of porosity to which the correlations are applied.

APPARATUS

The samples in the form of small disks with different porosities are manufactured in a specially designed steel mould by applying different pressures to the same amount of powder. An Amsler cupping machine permits the application of different loads ranging from 0 to 10 tons. The disks being manufactured are mounted in the so-called thermal conductivity [5] apparatus Fig. 1. In order to achieve low thermal resistance between the sample, the heat-sink and the heat-source all the contact areas are ground flat. Moreover, silicon grease is used between the contact faces for further reduction of the thermal resistance. In addition, a constant pressure was applied by means of a clamping device using a thin pyrex rod as a transducer. Heat losses by radiation from the sample surfaces are suppressed by a cylindrical radiation shield made of highly polished stainless steel. The e.m.f.s produced in the thermocouples are measured by FeuBuer potentiometer within approximately $\pm 1 \mu\text{V}$. The connections of the thermocouples to the potentiometer are made by using a 3-point switch with one common cold junction. This solves the technical problem which arises from the fact that the different cold junctions may not be exactly at the same temperature. The potentiometer indicator is a sensitive spot-galvanometer type L-217678 supplied by Cambridge with sensitivity 1 mA per 16 division.

EXPERIMENTAL PROCEDURE

1. Sample preparation

The powder was freed of all loosely adhering particles, any magnetic materials were removed by means of a magnet. Care was taken so that each sample was approximately uniform in particle size by passing it through a No. 100-sieve. Then, the powder was dried in an electric furnace to about 110°C for an hour before introducing into the hollow cylindrical part of the mould which was previously cleaned and dried. The piston of the mould was applied to the upper surface of the powder and a pressure ranging from 1 to 10 tons was applied to it using an Amsler Universal cupping machine. By this means disks of different porosities were produced.

2. Determination of porosity

The porosity greatly influences the weight of a body. For this reason the apparent density ρ_a of the disk must be known in addition to its true density ρ_s . The former is

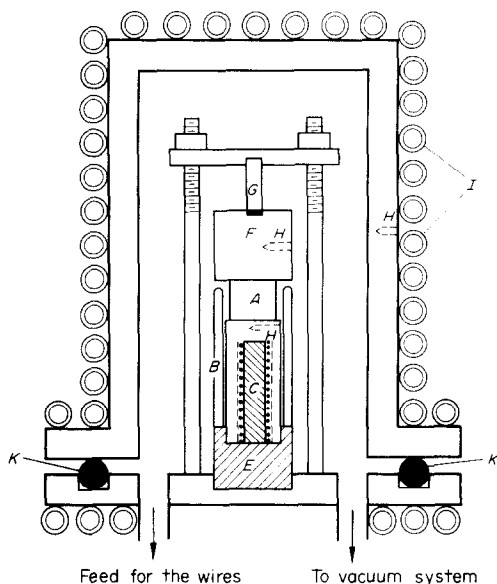


FIG. 1. Cross section of apparatus. A, sample; B, radiation shield; C, heater wire; E, transite (asbestos board); F, heat sink; G, pyrex rod; H, thermocouple holes; I, copper tubing; K, O-ring.

defined by $\rho_a = W/V$ and the latter is determined by a specific gravity bottle complying with the BS 2701. Thus, the porosity P (expressed as percentage of volume) is:

$$P = 100 \frac{V - V_s}{V} = 100 \frac{\frac{W_s + W_g}{\rho_a} - \frac{W_s}{\rho_s}}{\frac{W_s + W_g}{\rho_a}}$$

since $W_g \ll W_s$ it follows that:

$$P = 100 \frac{\rho_s - \rho_a}{\rho_s} = \left(1 - \frac{\rho_a}{\rho_s}\right) \times 100. \quad (1)$$

3. Calculation of the effective thermal conductivity

The emissivity of the heat sink was determined using a sample of known thermal conductivity and was found to be reproducible well within the experimental error ($\epsilon = 0.95 \pm 0.01$). The thermal conductivity values of different standard samples measured by the present method are proved to be reproducible within an accuracy better than 5 per cent of the reported values.

After the apparatus was assembled and evacuated, water was allowed to flow at constant temperature from a thermostat through the copper tubing. As soon as the temperature equilibrium was obtained (in about 4 h), the temperatures T_0 , T_1 and T_x were computed from the measured e.m.f.s. If heat losses by radiation from the sample surface are negligibly small the following equation holds:

$$\frac{A}{d} K(T_1 - T_x) = \sigma \epsilon S(T_x^4 - T_0^4).$$

The approach to steady-state was checked every 0.5 h and only the final temperatures were used in the calculations of the thermal conductivity.

EXPERIMENTAL RESULTS AND DISCUSSION

The results are represented graphically in Fig. 2. The graphical representation of the thermal conductivity against the solid phase volume fraction P_s for 29 different samples

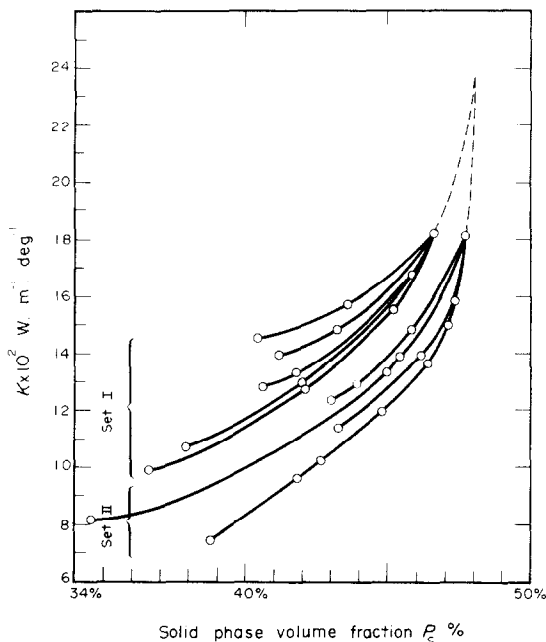


FIG. 2. K against P_s to show the thermal conductivity dependence on: 1—porosity; 2—pore-shape, -configuration and -orientation.

of the same material, manufactured at different conditions, shows interesting behaviour. For each value of P_s less than P_s equal to about 46 per cent, there are samples with different measured thermal conductivities although the constituent conductivities are the same. This indicates that the two phases within the samples are arranged in different manners, which clearly shows that the process of heat transmission through porous materials does not only depend on porosity, but also on the shape, configuration, and orientation of each phase relative to the other.

The experimental results lie in two sets of curves. In order to explain such a behaviour the authors assume that, each set corresponds to samples having the same pore-shape, while the points on each curve represent samples having the same pore-configuration, and -orientation. The convergence of the curves of each set to a point as P_s increases, illustrates the tendency of the thermal conductivity to approach the same value at a certain P_s . At this value of P_s the effect of pore-configuration, and -orientation on the thermal conductivity becomes negligible. Beyond this value, the dashed line shows the combined effect of both pore-shape and porosity alone. The two dashed lines meet at a point at which the main factor affecting the conductivity is the porosity.

CONCLUSION

As a result of this work, it could be concluded that, up to 48 per cent solid phase volume fraction, it is impossible—from the heat transfer point of view—to construct a model that represents reasonably well heterogeneous material. This means that any correlation, based on such a model, for predicting the apparent thermal conductivity will deviate from the measured conductivities to a certain degree. Such deviation decreases as P_s increases.

A second conclusion could also be drawn regarding the homogeneity of temperature inside the enclosure. It was proved that for the sake of uniformity of the heat energy transmission through walls insulated by units of insulating materials (e.g. fire bricks), such material should be manufactured with porosity not greater than 52 per cent (i.e. $P_s \geq 48$ per cent). This ensures that all the insulating units will have nearly the same thermal conductivity.

REFERENCES

1. A. Eucken, *Wärmeleitfähigkeit Keramischer feuerfester stoffe; Berechnung aus der Wärmeleitfähigkeit der Bestandteile*, *Forsch. Geb. IngWes.* B3 353, 16 (1932).
2. I. I. Sherif, The relationship between bulk density and thermal conductivity in refractory insulating bricks, *Silicates Industriels* 28(7-8), 1-2 (1963).
3. R. G. Diessler and G. S. Boegil, An investigation of effective thermal conductivity of powders in various gases, *Trans. Am. Soc. Mech. Engrs* 80, 1417 (1958).
4. S. C. Cheng and R. I. Vachon, The prediction of the thermal conductivity of two and three phase solid heterogeneous mixtures, *Int. J. Heat Mass Transfer* 12, 249-264 (1969).
5. G. Haacke and D. P. Spitzer, Method for thermal conductivity measurements on solids, *J. Scient. Instrum.* 42, 702-704 (1965).

Int. J. Heat Mass Transfer. Vol. 19, pp. 229-231. Pergamon Press 1976. Printed in Great Britain

ANALYSIS OF MIXED CONVECTION ABOUT A HORIZONTAL CYLINDER

E. M. SPARROW and L. LEE

Department of Mechanical Engineering, University of Minnesota, Minneapolis, MN 55455, U.S.A.

(Received 18 February 1975 and in revised form 7 April 1975)

NOMENCLATURE

D ,	cylinder diameter;
Gr_D ,	Grashof number, $g\beta(T_w - T_\infty)D^3/\nu^2$;
g ,	acceleration of gravity;
h ,	local heat-transfer coefficient;
k ,	thermal conductivity;
Nu ,	Nusselt number, hR/k ;
Nu_0 ,	hR/k at stagnation point;
Nu_x ,	Nusselt number, hx/k ;
Pr ,	Prandtl number;
q ,	local heat flux;
R ,	cylinder radius;
Re_D ,	Reynolds number, $U_\infty D/\nu$;
Re_x ,	Reynolds number, Ux/ν ;
T_w ,	wall temperature;
T_∞ ,	free stream temperature;
U ,	local free stream velocity;
U_x ,	velocity of approach flow;
u_i ,	coefficients, equation (1);
X ,	dimensionless coordinate, x/L ;
x, y ,	coordinates.

Greek symbols

β ,	thermal expansion coefficient;
ν ,	kinematic viscosity;
ϕ ,	angular coordinate;
Ω ,	mixed convection parameter, equations (6) and (7).

INTRODUCTION

HEAT transfer from horizontal cylinders under conditions of combined forced and natural convection flow has been the subject of numerous experimental studies, and [1-7] are representative of the available literature. On the other hand, aside from correlation efforts, there appears to have been little analytical study of the problem. Although the general case of mixed convection about a heated horizontal cylinder situated in an arbitrarily oriented forced convection flow is not readily amenable to analysis, it is possible to obtain solutions for a less general version of the problem. As will be demonstrated here, the case of an isothermal heated cylinder in a vertical forced convection upflow can be solved provided that a boundary-layer region exists. This fact was recognized by Acrivos [8], who obtained the $Pr \rightarrow 0$ and $Pr \rightarrow \infty$ limits for the Nusselt number at the lower stagnation point.

*In those cases, similarity may be achieved if contrived boundary conditions are employed.

It is well established that for both forced convection and natural convection, a boundary-layer flow will exist on the lower part of the cylinder for moderate and large values of the Reynolds and Grashof numbers. Such a boundary-layer flow should also exist for mixed convection under aiding conditions.

For the isothermal cylinder, the separate forced convection and natural convection boundary layers possess an interesting common characteristic, namely, that they both have the same dependence on the streamwise coordinate (measured from the lower stagnation point). Consequently, the corresponding mixed convection problem retains this same streamwise dependence. Therefore, the mixing of the two forms of convection is not, in itself, the cause of boundary-layer nonsimilarity. This outcome is in contrast to mixed convection problems for other geometries such as horizontal plates and vertical plates and cylinders, where the mixing of the two flows causes nonsimilarity.*

ANALYSIS

A schematic diagram of the horizontal cylinder problem showing coordinates and nomenclature is given in Fig. 1. The boundary-layer flow is driven both by the external pressure gradient dp/dx due to the free stream velocity of the forced convection and by the buoyancy force $g\beta\rho(T - T_x)\sin\phi$. Via Bernoulli's equation, the pressure gradient is replaced by $-\rho U(dU/dx)$, where U is the local free stream velocity which, for a cylinder, can be represented by

$$U = u_1(x/R) + u_3(x/R)^3 + u_5(x/R)^5 + \dots \quad (1)$$

The constants u_1, u_3, u_5, \dots differ from those for potential flow due to displacement of the streamlines which results from boundary-layer separation. Values measured by several investigators are given in [9]. For the buoyancy term, the expansion of the $\sin\phi$ factor, with $\phi = x/R$, is

$$\sin\phi = (x/R) - (1/6)(x/R)^3 + (1/120)(x/R)^5 + \dots \quad (2)$$

Inspection of equations (1) and (2) suggests the similarity of the x -dependence of the two force components which drive the boundary-layer flow, and this may be confirmed by a complete evaluation of the respective terms.

The first term of the respective series (1) and (2) pertains to the lower stagnation point. If the conventional constant property momentum equation and non-dissipative energy equation are used, with the aforementioned pressure and buoyancy forces as inputs to the former, and a similarity